Analytical and numerical performance models of a Heisenberg Vortex Tube

C D Bunge, K A Cavender, K I Matveev, and J W Leachman

HYdrogen Properties for Energy Research (HYPER) Laboratory, Washington State University, Pullman, WA 99164-2920 USA

Corresponding author. *Email address:* jacob.leachman@wsu.edu

Abstract. Analytical and numerical investigations of a Heisenberg Vortex Tube (HVT) are performed to estimate the cooling potential with cryogenic hydrogen. The Ranque-Hilsch Vortex Tube (RHVT) is a device that tangentially injects a compressed fluid stream into a cylindrical geometry to promote enthalpy streaming and temperature separation between inner and outer flows. The HVT is the result of lining the inside of a RHVT with a hydrogen catalyst. This is the first concept to utilize the endothermic heat of para-orthohydrogen conversion to aid primary cooling. A review of 1st order vortex tube models available in the literature is presented and adapted to accommodate cryogenic hydrogen properties. These first order model predictions are compared with 2-D axisymmetric Computational Fluid Dynamics (CFD) simulations.

1. Introduction

Many fundamental theories have attempted to model the energy separation mechanism that drives the Ranque-Hilsch Vortex Tube (RHVT) [1, 2]. This "tornado"-generation device operates similarly to a rotor-less turbo-expander by converting fluid power into cylindrical kinetic energy. This kinetic energy has a substantial gradient which radially streams enthalpy to generate a temperature difference between inner and outer flows that are extracted on either end of the tube. The Heisenberg Vortex Tube (HVT) is a new concept that modifies the RHVT specifically for cryogenic hydrogen by incorporating a para (p) to ortho (o) hydrogen conversion (p-o) catalyst on the inner wall of the centrifuge. The HVT is based on the most common counter-flow RHVT configuration and is shown in figure 1 below.

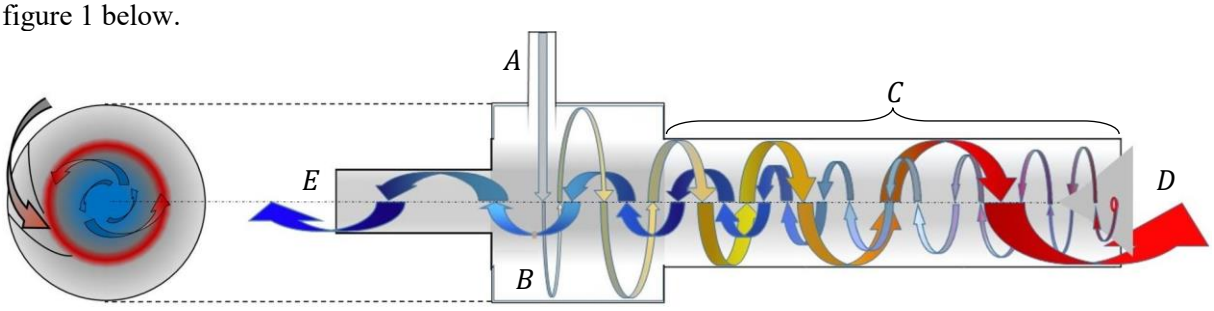

Figure 1. Conceptual schematic of a counter-flow Heisenberg Vortex Tube (HVT): A. Inlet injection plenum, B. Vortex Generator, C. Centrifuge with catalytic liner, D. Hot annular plug outlet, E. Cold centerline diffuser.

This catalyst, allows for the endothermic heat of p-o conversion to improve cooling performance beyond that of a conventional RHVT. To predict performance gains from the HVT concept an extended heat exchanger model is presented and compared to other empirical and semi-empirical models that are adapted to cryogenic hydrogen. Following this we present a validated CFD code adapted for operating with REFPROP integrated cryogenic hydrogen properties. We conclude with a comparison of the models operating with cryogenic hydrogen at an inlet temperature of 77 K and show preliminary comparisons to initial experimental measurements in a companion publication.

2. Overview of 1st Order Vortex Tube Models

Since the discovery of the vortex tube there have been many theories which attempt to describe the theoretical energy migration mechanism which cools the inner and heats the outer flow. The original pioneers who studied the phenomena relied on experimental iteration to connect flow geometries with simplified fluid properties for the first predictive models [3]. We primarily restrict this overview to models developed over the last two decades.

J.G. Polihronov and A.G. Straatman (2012) modeled the vortex tube by isolating the centrifugal effects on a rotating fluid in an adiabatic duct [4]. A second law efficiency was obtained from Eiamsa-ard and Provonge (2008) to gain insight into the ideal performance of the vortex tube. [5]. Another vortex tube modelling approach by Ahlborn and Gordon (2000) is to account for secondary flow by analogy with a heat pump [6]. Another model from Liew et al. (2012) explains that the fundamental heat transfer mechanism is due to radial pressure gradient heat pumping by turbulent eddies which are compressed and expanded in outer and inner flows [7].

However, the semi-empirical models above were derived with air at room temperature. Cryogenic hydrogen can exhibit non-ideal behaviour and thus presents a need for additional model considerations. Moreover, fluid properties can vary significantly within the vortex tube itself, especially in the case of a reacting para-orthohydrogen flow, creating the need for spatial resolution of properties and higher order models.

An Extended Heat Exchanger (EHE) model of a counter-flow heat-exchanger was implemented by Nellis and Klein (2002) which originated from Lewins et al. (1998) [8, 9]. This model introduced fluid properties in a quasi-1D outer and inner flow scenario.

3. Adaptation of the EHE Model for Cryogenic Hydrogen

The EHE model accounts for turbulent heat pumping from the inner to outer flow under a pressure gradient. The inner flow cross-section is approximated as a forced turbulent vortex and the radial heat pumping is driven by turbulent fluctuations of fluid particles in the presence of a pressure gradient. The energy balance for the inner flow is modeled as:

$$\dot{m}_i c_p \frac{dT_i}{dx} = -\dot{q}_{io} \tag{1}$$

Where the term of the left is the temperature differential, the first term on the right represents the turbulent heat transfer as in equation (3) below. The enthalpy streaming is a result of particle transport from a higher or lower pressure region as it contracts or expands. The energy balance is similar to the outer flow with the addition of the p-o conversion term. The energy balance for the outer flow is:

$$\dot{m}_o c_p \frac{dT_o}{dx} = \dot{q}_{io} - \dot{m}_{po} A_{vt} \Delta h_{po} \tag{2}$$

The last term represents the p-o conversion which causes an endothermic reaction in the outer flow where current conversion units measure per area, A_{vt}, of catalyst. Methods for calculating the enthalpy of formation for p-o conversion are described elsewhere [10]. Investigation of the p-o transition catalysis mechanisms on a molecular level reveals why the near supersonic azimuthal vortex tube flow boosts catalyst performance. The two main factors which dictate the probability for a para molecule to

transition into the ortho- state are the kinetic energy which the molecule impinges on the catalyst and the spatial interaction with the catalyst perturbation mechanism. Molecular hydrogen has the potential to stick or become physisorbed to a catalyst surface [11]. However, the proton-perturbation distance has the most influence on the conversion rate which changes at the distance raised to the eighth and sixth powers in two separate models [12]. There is also an optimum surface residence time for a molecule to conduct the p-o conversion energy. This time typically increases with decreasing temperature. Therefore, the conversion mechanisms at work in the high shear and turbulent flow of the hydrogen in the vortex tube have potential to enable fast transitions through intense interaction and mixing. As the catalyst interacts with the high shear boundary layer the equilibrium o-p fraction is shifted to favor a higher orthohydrogen fraction due to the increased temperature. To estimate the converted mass flow rate, $\dot{m}_{po}$, the percentage of conversion is modeled by the conversion potential:

$$\beta^{cp} = \frac{Maximum\ p-o\ conversion\ percentage}{Estimated\ p-o\ conversion\ percentage} \tag{3}$$

Thie conversion potential in equation (3) provides a benchmark metric which allows simple comparison of various catalyst performance. The specific metric indicates that the performance of the catalyst approaches the ideal max conversion value at $\beta^{cp} = 1$ given that the max possible conversion potential lowers as the cold flow fraction increases. [12]. A mixture of equilibrium hydrogen will lack a conversion potential without a temperature differential. The equilibrium orthohydrogen fraction at an inlet of 77K is approximately 49.4%. This equilibrium ortho-hydrogen fraction increases to approximately 55.5% at the EHE predictive outer wall temperature. Therefore, the maximum para-ortho hydrogen conversion percentage is 6.1%. We can estimate the power extraction possible given the para-orthohydrogen enthalpy of conversion of 683 kJ/kg at an average of 81 K and total mass flow rate of 0.15 g/s. This power extraction equals approximately 5 W in addition to the fluid mechanical cooling power of 43 W. The $\dot{q}_{io}$ term in equation (2) represents the turbulent heat transfer model under a radial pressure gradient from inner to outer flows:

$$\dot{q}_{io} = -c_p \rho l^2 \frac{dV}{dr}\left[\frac{dT}{dr} - \left(\frac{dT}{dP}\right)_s \frac{dP}{dr}\right] \tag{4}$$

Where c_p is the specific heat at constant pressure, ρ is density, l is the turbulent mixing length, T_m, P_m are the mean temperature and pressure in the mixing length model. The principle behind this model is that a particle absorbs or rejects heat when its temperature due to expansion or compression in the 2nd term becomes different than the local temperature in the 1st term. The model assumptions include isentropic compression and expansion when turbulence causes random shifts in the radial direction. Another empirically derived parameter is the pressure at the hot end which is contributed by 1/3 of the PR and 2/3 of the pressure at the cold end. REFPROP fluid properties have been implemented as well. Overall performance is sensitive to the isentropic nozzle efficiency and is set at 95%. Fitting parameters include turbulent mixing length, returning flow fraction, and tangential velocity decay [13].

The model is solved for the temperature of both the hot and cold through the specification of a cold flow fraction, inlet temperature, pressure ratio. A forward-time Crank-Nicolson finite difference scheme is used to solve for the temperatures of both inner and outer flows. Figure 3 shows the effect of catalyst activity on HVT performance.

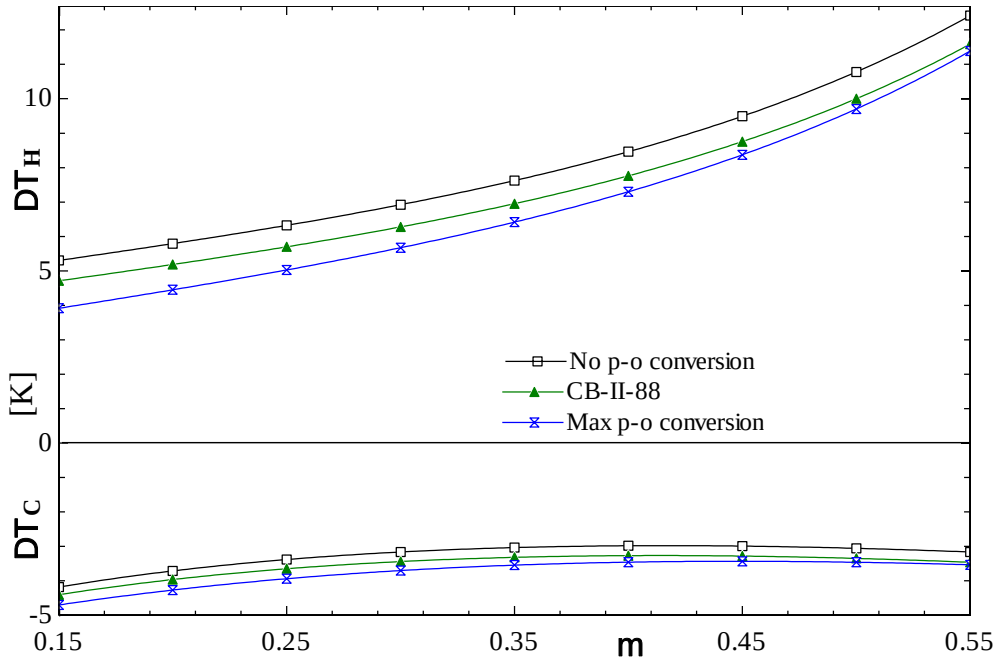

Figure 3. Plot of temperature drop versus cold flow fraction at various conversion rates at a $PR = 2$. Equilibrium conditions are associated with the p-o heat of conversion potential at the hot outlet. μ is the cold flow fraction. ΔT_C is the differential in cold outlet to reservoir temperature K ΔT_H is the differential in total temperature from hot outlet to reservoir in K).

With a perfect catalyst present, the cold end temperature is projected to improve 10%. The addition of experimentally measured CB-II-88 by Brooks et al. shows a $\beta^{cp} = 2.35$ at $\mu = 0.15$ and $\beta^{cp} = 1.25$ at $\mu = 0.55$. What this model ultimately reveals is an inverse of typical concave cold flow fraction versus cold end temperature [2]. There is typically a decrease in cold end temperature drop at higher cold flow fractions. However, this indicates an increase in efficiency at higher cold flow fractions which is due to the axial shear work transfer. Previous studies have shown that the axial shear work transfers the sensible heat from the outer flow into the inner flow which reduces total energy separation. However, with hydrogen, the inner - outer shear boundary layer is close to the outer wall which reduces this effect.

Ultimately, even the spatially resolved EHE model makes aggressive assumptions regarding the turbulent mixing length and enthalpy streaming. Comparisons with Computational Fluid Dynamic models of the HVT can help to validate these assumptions.

4. Computational Fluid Dynamic Models of Vortex Tubes

Computational Fluid Dynamic (CFD) packages have renewed interest in the RHVT. We briefly overview some of the most recent studies. Aljuwayhel et al. modeled a vortex tube with a Re-Normalization Group (RNG) and standard $\kappa - \omega$ solver in ANSYS FLUENT® [14]. A Large Eddy Simulation (LES) code was used by T. and B. Farouk to model the vortex flow [15]. T. Dutta compared a 3D simulation to an axisymmetric 2D mesh and noted the temperature differential was very small [16]. As with the air-derived 1st order models these studies primarily focus on the room temperature regime. However, the application of a cryogenic vortex tube for two-phase liquid oxygen extraction has been investigated [17, 18].

A 2D axisymmetric model with swirl is based on a vortex tube geometry which was validated with air at room temperature [19]. The mesh of the 2D model converges at a total node count of 99,693 to produce consistent results and avoid unnecessary computational cost. In order to adjust performance parameters, the hot and cold exit pressures determined the cold flow fraction and pressure ratio, respectively. This model uses a standard RANS based $\kappa - \omega$ turbulence solver with compressibility effects that has been previously implemented with success [19]. The fluid properties of equilibrium

normal-hydrogen were implemented through REFPROP with the density-based solver at 77 K. Effective mass and energy errors are less than 0.5% for the model shown below.

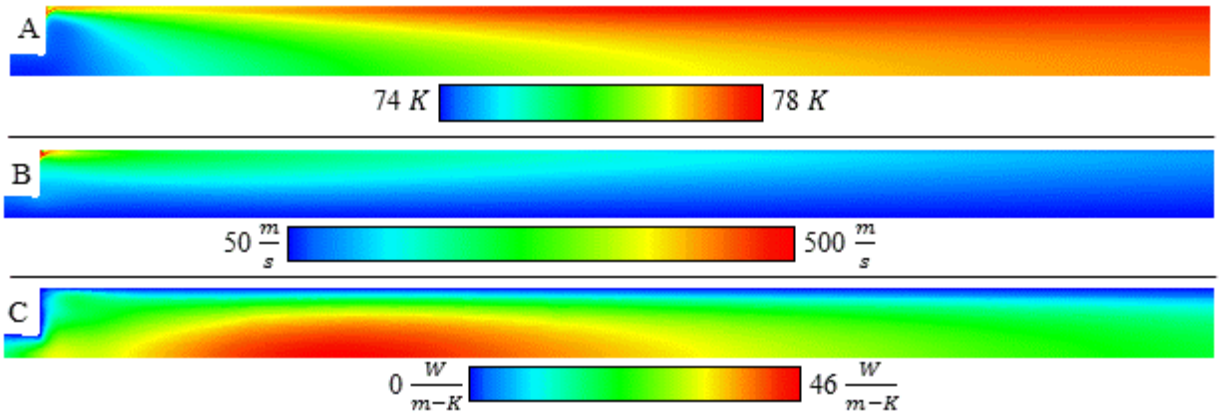

Figure 4. Performance plots of 2D axisymmetric CFD model with REFPROP integrated. Inlet and cold end on left and hot end further downstream on right. PR = 1.73, μ = 0.37. A. Total temperature contour. B. Tangential swirl velocity. C. Effective thermal conductivity.

This model shows an intense tangential velocity at the inlet which sharply transitions into a free vortex near this region and confirms the tangential shear force as the main energy separation mechanism. This then transitions into a forced vortex wake region which conducts heat from the center of the vortex tube to the outer wall as see in figure 4, C. The plots in figure 4 above also show a distinct reduction in the heat transfer from inner to outer flow as the tangential swirl velocity decays. However, lighter molecular weight working fluids have shown to produce higher temperature separations [16]. This may be due to the sharp tangential velocity gradient near the inlet which enables a discrete turbulent wake region which enable turbulent heat transfer fluctuations.

5. Comparisons of Models to Experimental Measurements

The 1st order literature-derived models as well as the EHE and CFD models above provide a broad look at the performance potential of the HVT. In a companion publication, we have also conducted an experimental sweep of an HVT with and without catalyst [13]. The cold flow fraction of 0.37 with some experimental measurements slightly above that mark as seen in table 1. Figure 5 below shows there is relatively good agreement with low pressure ratio model predictions and experimental results.

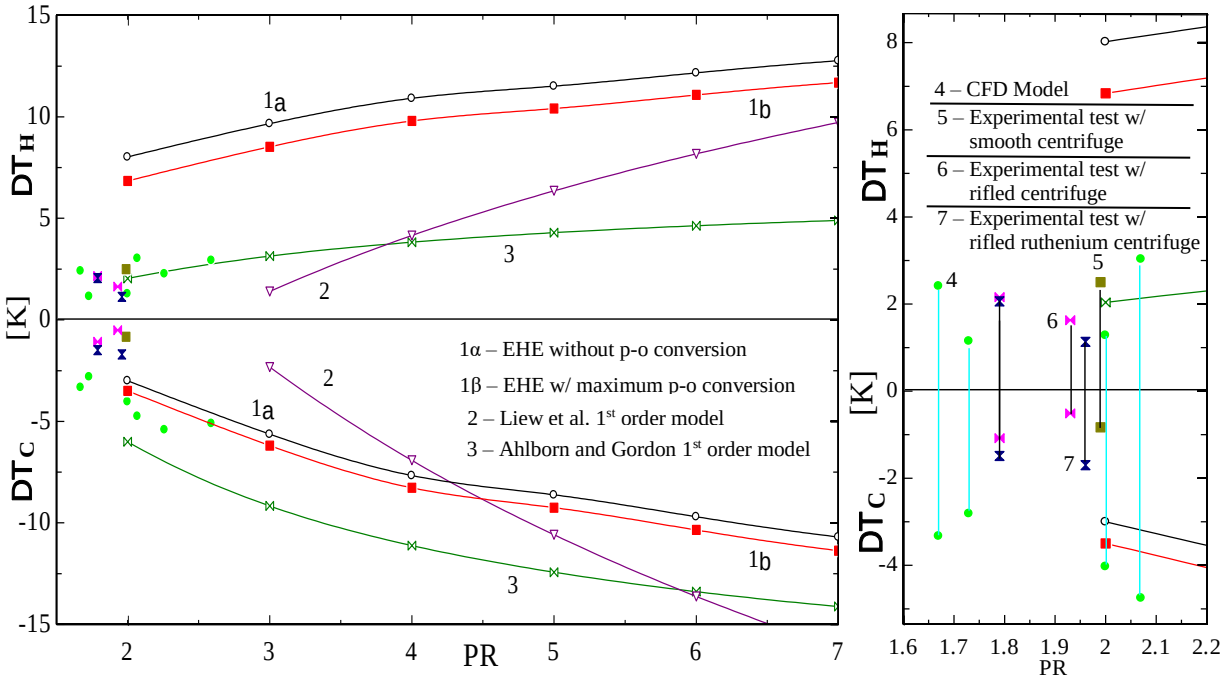

Figure 5. Temperature separation performance comparison of 1st order models, 2D axisymmetric CFD model, and experimental measurements with and without zoom perspectives. Where 1α represents the EHE model without p-o conversion, 1β - EHE model with maximum p-o conversion potential, 2 – Liew et al. [7] model, 3 – Ahlborn and Gordon [6] model, 4 - 2D CFD model ($\mu = 0.37 \pm 0.035$), 5 – HVT experimental test w/ smooth centrifuge, 6 – HVT experimental test w/ rifled centrifuge, 7 – HVT experimental test w/ rifled ruthenium centrifuge. PR is Pressure Ratio of the total stagnation pressure of the upstream reservoir to total stagnation of the cold end outlet.

While all other geometrical ratios are held constant, the L/D ratio is another parameter which varies between models. The EHE is similar to historical values at 50 and the 2D axisymmetric CFD model is 20. This suggests that the energy separation can occur despite a short turbulent wake fluctuation collapse.

Another important comparison is the temperature separation at cryogenic temperatures compared to room temperatures. As seen in table 1 on the next page, this is linked to the reduced enthalpy available in cryogenic hydrogen. The first order and experimental results suggest a link between turbulent wake fluctuation and enthalpy of the system. The bulk majority of enthalpy streaming occurs within the first 5 diameters whereas air requires 30 or more [16, 19].

Historical experimental tests by A.F. Johnson and Elser and Hoch suggest the geometrical parameters of the tube are important. As noted above, the higher cold flow fraction suggests an improvement in performance. Though, there was a decrease in performance with high cold flow fraction with an air-tuned cold flow fraction of 0.61 [20]. Elser and Hoch, on the other hand, produced an approximately 20% greater performance with H_2 than Argon, Air, CH_4, and CO_2, despite having a similar ratio of specific heats [21, 22].

Table 1. Review of H_2 vortex tube studies.

		Analysis type		Results[a]					
Report	Year	Fluid	Method	PR	T_R	ΔT_C	ΔT_H	ΔT_{Total}	μ
A.F. Johnson	1947	normal-H_2	Experimental	6.6	294	-15.9	-	-	-
Elser and Hoch	1951	normal-H_2	Experimental	6	285	-	-	74	0.5
T. Dutta et al.	2013	normal-H_2	FLUENT®	3	115	-10	25	35	0.22
			w/REFPROP	3	115	-7	9	16	0.54
Bunge et al.	2017	normal-H_2	FLUENT®	1.73	77	-2.81	1.15	3.96	0.36
			w/REFPROP	2	75	-6.41	0.46	6.87	0.70
Shoemake et al.	2017	para-H_2	Experimental						
			w/o catalyst	1.79	73	-1.08	2.16	3.24	0.37
			w/Ruthenium	1.96	74	-1.70	1.13	2.83	0.42

[a]Where T_R is temperature of the reservoir (inlet fluid) before centrifugal acceleration (K), ΔT_{Total} is the total differential in total temperature from hot outlet to cold outlet. Each row corresponds to the respective method.

6. Conclusions

An Extended Heat Exchanger model has been adapted to account for non-ideal cryogenic hydrogen properties. The model shows that para-orthohydrogen conversion along the tube wall can increase vortex tube performance 10 % at a pressure ratio of 2 and inlet temperature of 77 K compared to traditional Ranque-Hilsch vortex tubes while suggesting a higher cold flow fraction has the potential to improve performance and efficiency. These model predictions were compared to Computational Fluid Dynamic simulations of a vortex tube operating with cryogenic hydrogen completed in ANSYS with REFPROP and experimental measurements. The extended heat exchanger model overpredicts the temperature separation, primarily the temperature rise, occurring at low pressure ratios. Further experimental measurements are planned to test the model accuracies at higher pressure ratios and colder temperatures.

References

[1] Ranque G 1933 Expériences sur la détente giratoire avec productions simultanées d'un echappement d'air chaud et d'un echappement d'air froid *J. Phys. Radium* **4**

[2] Hilsch R 1947 The use of the expansion of gases in a centrifugal field as cooling process *Rev. Sci. Instrum.* **18**

[3] Westley R 1954 A bibliography and survey of the vortex tube. Canfield College of Aeronautics)

[4] Polihronov J G and Straatman A G 2012 Thermodynamics of angular propulsion in fluids *Phys. Rev. Lett.* **109**

[5] Eiamsa-ard S and Promvonge P 2008 Review of Ranque–Hilsch effects in vortex tubes *Renew. Sust. Energ. Rev.* **12** 1822-42

[6] Ahlborn B and Gordon J 2000 The vortex tube as a classical thermodynamic refrigeration cycle *J. Appl. Phys.* **88** 3645-53

[7] Liew R, Zeegers J C H, Kuerten J G M and Michalek W R 2012 Maxwell's demon in the Ranque-Hilsch vortex tube *Phys. Rev. Lett.* **109**

[8] Lewins J and Bejan A 1999 Vortex tube optimization theory *Energy* **24** 931-43

[9] Nellis G F and Klein S A 2002 The application of vortex tubes to refrigeration cycles. In: *Internaltional Refrigeration and Air Conditioning Conference,*

[10] Leachman J W, Jacobsen R T, Lemmon E W and Penoncello S G 2017 *Thermodynamics Properties of Cryogenic Fluids*: Springer)

[11] Fukutani K and Sugimoto T 2013 Physisorption and ortho-para conversion of molecular hydrogen on solid surfaces *Prog. Surf. Sci.* **88** 279-348
[12] Brooks C J, Wang W and Eyman D P 1994 Supported transition metal catalysis for para- to ortho- hydrogen conversion. Lewis Research Center) pp 1-106
[13] Merkulov A P 1969 Вихревой эффект и его применение в технике (Vortex effect and its technical application) *Mashinostroenie, Moscow*
[14] Aljuwayhel N F, Nellis G F and Klein S A 2005 Parametric and internal study of the vortex tube using a CFD model *Int. J. Refrig.* **28** 442-50
[15] Farouk T and Farouk B 2007 Large eddy simulations of the flow field and temperature separation in the Ranque-Hilsch vortex tube *Int. J. Heat Mass Trans.* **50** 4724-35
[16] Dutta T, Sinhamahapatra K P and Bandyopadhyay S S 2013 CFD analysis of energy separation in Ranque-Hilsch vortex tube at cryogenic temperature *J. Fluids* **2013** 1-14
[17] Balepin V, Rosholt D and Petley D 1999 Progress in air separation with the vortex tube. In: *9th International Space Planes and Hypersonic Systems and Technologies Conference,*
[18] Hunt J L, Lockwood M K, Petley D H and Pegg R J 1997 Hypersonic airbreathing vehicle visions and enhancing technologies. (NASA Langely Research Center pp 1285-96
[19] Bej N 2015 Numerical studies on the performance enhancement of a Ranque-Hilsch vortex tube. In: *Department of Aerospace Engineering*: Indian Institute of Technology Kharagpur)
[20] Johnson A F 1947 Quantitative study of the Hilsch heat separator *Can. J. Res.* **25** 299-302
[21] Van Deemter J 1952 On the theory of the Ranque-Hilsch cooling effect *Appl. Sci. Res.* **3** 174-96
[22] Elser K and Hoch M 1951 Das verhalten verschiedener gase und die trennung von gasgemischen in einem wirbelrohr *Z. Naturforschg.* **6a** 25-31

Acknowledgements
This material is based upon work supported by the U.S. Department of Energy's Office of Energy Efficiency and Renewable Energy (EERE) under the Fuel Cell Technologies Office under project "Improved Hydrogen Liquefaction through Heisenberg Vortex Separation of para and orthohydrogen". This work was also supported by a NASA Space Technology Research Fellowship.